Hydraulic tomography in time-lapse mode for tracking the clogging effects associated with the colloid injection

Min Tan Vu, Abderrahim Jardani, Mohamed Krimissa, Pierre Fischer, Nasre Dine Ahfir

HAL Id: hal-02440558

https://normandie-univ.hal.science/hal-02440558

Submitted on 20 Jul 2022

Hydraulic tomography in time-lapse mode for tracking the clogging effects associated with the colloid injection.

M. T. Vu [1,*], A. Jardani [1], M. Krimissa[2] , P. Fischer[1], and N. Ahfir[3]

[1] Université de Rouen, M2C, UMR 6143, CNRS, Morphodynamique Continentale et Côtière, Mont Saint Aignan, France

[2] EDF Electricité de France, 6 Quai Watier, 78400 Chatou, France

[3] Université le Havre Normandie, UMR6294 Laboratoire Ondes et Milieux Complexes, Le Havre, France

Keywords: Hydraulic tomography, Time-lapse inverse problem, Joint inversion, Colloid injection, Colloid transport, Clogging

Key points:

- Numerical simulations were developed to highlight the effect of clogging on the hydraulic transmissivity.

- Inversion process was formulated in time-lapse mode to track the evolution of transmissivity field in time,

- Adjoint state formulation was used to derive the sensitivity matrices for the coupled problem.

Abstract

Clogging due to transport and accumulation of the colloids in the pore space has been recognized as one of the most significant challenges in water management research and environmental engineering. This paper proposes an inversion algorithm in time-lapse mode to track that complex process through the assessment of alteration in the transmissivity field produced by the injection of colloids. The concept is based on a joint inversion of hydraulic head and colloidal particles concentration data acquired during the injection of colloids in the porous aquifer to reconstruct the spatial variability of the transmissivity field at different times. The inversion code is deterministic and was implemented in the time-lapse scheme by adding in the objective function a temporal geostatistical constraint to control changes of the hydraulic transmissivity. This algorithm is linked to a forward problem that consists of the groundwater flow and transport equations, which were solved numerically and jointly by considering the effect of particles deposition on the decrease of hydraulic properties. As the inverse problem is deterministic and underdetermined, we have opted to use the efficient adjoint state technique to derive the sensitivity matrices. The approach has been successfully applied to a theoretical case in which the hydraulic head responses have been used alone and jointly to assess the evolution of the clogging impact on hydraulic transmissivity.

1. Introduction

For decades, the understanding of the mechanisms of colloidal particle migration in porous or fractured aquifers has aroused the interest of geoscientists; especially for addressing certain issues that may affect the sustainability of the exploitation of groundwater resources, such as clogging and turbidity phenomena (Jeong, et al., 2018). Clogging is one of the main causes of damage to the productivity of groundwater wells, by reducing the hydraulic conductivity of the soil surrounding the wells. Because of the mobilization and then the retention of the colloidal particles, which may imply a costly rehabilitation operation, or early abandonment of wells (De Zwart, 2007). The turbidity of the groundwater is mainly associated with an instantaneous and highly dynamic transport of fine particles during rainfall events on the karstic catchments, where the sinkholes and karstic conduits facilitate the introduction, resuspension, and the mobility of particles in the subsurface (Pronk, et al., 2009).

Recently, the interest of the geoscientists has shifted to the comprehension of the role of colloidal particles in the spreading of organic and inorganic contaminants in the subsurface to address the environmental issues related to anthropogenic contamination of water resources. The studies focus on the main underlying mechanisms that control the migration of particles such as: the chemical nature of the colloids and interstitial water (ionic strength and pH); the chemical interactions between the contaminants (organic or inorganic) and colloids; the concentration of the colloids in the soil; and the water velocity that depends on the hydraulic conductivity of the soil (McCarthy & McKay, 2004; Sen & Khilar, 2006; Flury & Qiu, 2008). Among these works: Saiers and his co-authors who focused on studying the effect of colloidal particles on the transport of contaminants such as Hydroxyatrazine and Cesium through sand column experience (Saiers & Hornberger, 1999; Cheng & Saiers, 2009). Short et al., 1988 showed that the colloidal particles rich in Fe and Si have a high ability to accelerate the migration of the Uranium and the Thorium species (Short, et al., 1988). Ribeiro et al. 2014 discussed the role of the colloidal particles in the E. coli bacteria transfer into a karstic aquifer during rainy events. Abdel-Salam and Chrysikopoulos, 1995 proposed a mathematical approach to numerically simulate the transport of colloids in the fractured medium.

Other works have treated the transfer modalities of active colloids, such as the Nanoscale zero-valent used as cleaning agents for aquifers contaminated with chlorinated hydrocarbons (Mueller, et al., 2012). (Strutz, et al., 2016). The effectiveness of these injected active colloids strongly depends on the hydraulic conditions around the injection well, and its clogging can block the operation of rehabilitation. By contrast, in some situations, the clogging may be a positive measure to prevent leakage of contaminants (Persoff, et al., 1995). In that regard, the artificial injection of colloids can be considered as an alternative to limit the spreading of pathogenic microorganisms or radioactive substances(Peterson, 1994) (IAEA, 2001).

In general, the clogging of the porous medium results from a complex combination of physical, chemical and biological processes that manifests itself through a decrease in the hydraulic conductivity of the soil. (Torkzaban, et al., 2015) (Sharma & Yortsos, 1987). We believe that the monitoring of these hydraulic properties changes associated with clogging can become a paramount gait in designing of remediation techniques.

In this manuscript, we present and discuss the pertinence of an inversion algorithm formulated in time-lapse mode to follow the spatio-temporal evolutions of the clogging driven by a colloidal injection in a confined aquifer. Inverse algorithms have been broadly applied during the last decades, in the modeling of groundwater flows and particularly to image the spatial variability of hydraulic conductivity in 3D or transmissivity in 2D (Zimmerman, et al., 1998; Yeh, 1986; Kitanidis, 1996). This spatial imaging of hydraulic parameters is known as hydraulic tomography, which results from the cross-interpretation of a set of piezometric data collected during multiple pumping tests using an inversion algorithm (Soueid, et al., 2015). However, to our knowledge, this method is not yet extended to time-lapse inversion by combining spatio-temporal data to bring out the dynamic changes of hydraulic properties caused by clogging processes.

Time-lapse inversion scheme is commonly applied in the geophysics discipline to study the dynamic change of physical properties (such as : electrical conductivity, and dielectric constant) in the subsurface, associated for instance with: water infiltration, salt water intrusion (Hermans, et al., 2012), salt tracer experiment (Johnson, et al., 2010; Karaoulis , et al., 2011; Jardani, et al., 2013) and temperature changes (Legaz, et al., 2009).

In this paper, we formulate a hydraulic tomography algorithm in time-lapse form to image spatio-temporal variations in the transmissivity field that occurred during the injection of colloids by inverting the hydraulic head data alone or jointly with the colloid concentrations. These data are obtained by solving numerically and sequentially a coupled system of groundwater flow and transport equations, built in a way to reproduce a temporal change in the hydraulic transmissivity of a confined aquifer via colloidal injections on several wells. The hydraulic head and concentrations data recovered on virtual piezometers at different instants indirectly reflect the evolution of hydraulic conditions of the aquifer during the injections. The inversion of these data relies on a deterministic and nonlinear algorithm in which the sensitivity matrices (also called Jacobian matrices) connecting the transmissivity field, considered here as unknown parameters, and the numerical data are computed from the adjoint state formulations.

The efficiency and the limit of this algorithm are revealed by its application to theoretical cases. In the first case, we survey in 2D the change of transmissivity field over time using only the hydraulic head data in the time-lapse inversion algorithm. However, in the second case, we use the same data, but this time, the inverse formulation does not take into account the time-lapse term, which allows us to include in the inverse process the dynamic effect. In the last case, we investigate the efficiency of the combination of the hydraulic and concentration data in the monitoring of transmissivity changes.

2. Theoretical Background

In this section, we introduce the equations governing the transport of colloidal particles in a heterogeneous porous media in 2D. The equation system consists of the groundwater flow and transport equations solved numerically in iterative mode by using a finite element approach and considering the effects of colloids injection on the variation of the hydraulic conductivity during the transport process.

2.1 Colloid Transport

The macroscopic transport equation can be derived from mass balance of colloids over a representative element volume (REV) in the medium. Three main mechanisms control the evolution of the system, including convective flow, hydrodynamic dispersion and colloid suspended mass exchange through attachment and detachment processes on the fluid-solid interfaces. The transport in the aqueous phase, hence, can be described by an advection-dispersion form (Sun, et al., 2001; De Marsily, 1986).

$$\frac{\partial c}{\partial t} = \nabla . \boldsymbol{D} \nabla c - \nabla . (\boldsymbol{v} c) + R, \tag{1}$$

where c represents the colloid concentration in the aqueous phase (mol/m^3), t is the time (s), $\boldsymbol{D}$ denotes the particle hydrodynamic dispersion (m^2/s) and $\boldsymbol{v}$ is the particle velocity (m/s). R is the colloid mass change related to the attachment and detachment (mol/m^3/s).

2.2 Colloid Attachment and Detachment

Generally, the variation of colloid mass is expressed in terms of the attachment and detachment of particles in the pore space that have been widely formulated in the transport equation under a linear kinetic forms (Gruesbeck & Collins, 1982; Civan & Nguyen, 2005; Civan, 2016; Lohne, et al., 2010; Wang S. & Civan F., 2005a; Wang & Civan, 2005b). The attachment is supposed proportional to the concentration of colloids in the aqueous phase as (Gruesbeck & Collins, 1982)

$$R_{attach} = -K_d c, \tag{2}$$

where R_{attach} (mol m^{-3} s^{-1}) is the attachment rate, K_d (1/s) refers to the attachment coefficient, which can vary in time and space, and depends on the water velocity, pore size and other physico-chemical properties of matrix (such as: pH, zeta potential, temperature, etc.) (Ikni et al. 2013) (Civan, 2016). Commonly, this parameter is inferred from the adjustment of experimental clogging data, and the estimated values most often vary between 1x 10^{-3} – 5x 10^{-2} (1/s) (Zheng et al 2014).

In the literature, there are many forms to express detachment rate in function of water velocity, among them (Gruesbeck & Collins, 1982; Wang S. & Civan F., 2005a; Wang & Civan, 2005b; Lohne, et al., 2010):

$$R_{detach} = \begin{cases} \alpha \, \varepsilon \, (v - u_c) & v > u_c \\ 0 & v \leq u_c \end{cases} \quad , \tag{3}$$

where the detachment occurs only when the local fluid velocity overpasses a critical velocity u_c that can vary between 0.05 to 0.1 (cm/s) according to the experimental data (Gruesbeck & Collins, 1982; Reddi, et al., 2000). The removal mass is proportional to the net volume occupied by the particles $\varepsilon = \phi - \phi_0$; ($\phi$ and ϕ_0 are the instantaneous and initial porosity of the medium, respectively). α denotes the constant rate detachment that can be reformulated as function of Ionic strength of water (Gruesbeck & Collins, 1982; Wang S. & Civan F., 2005a; Wang & Civan, 2005b; Lohne, et al., 2010)..

Once the two phenomena, attachment and detachment, are simultaneously considered, that produces

$$R = R_{attach} + R_{detach}. \tag{4}$$

In this study, the seepage velocity in the medium is much smaller than the critical velocity, thus the detachment is negligible.

Under the influence of colloid kinetics, the spatial distribution of porosity evolves in time, corresponding to the attachment and detachment processes, by

$$\frac{d\phi}{dt} = \frac{M}{\rho_s} R, \tag{5}$$

with ρ_s is the solid density, close to 2600 kg/m^3, M is the molar mass of colloids (kg/mol).

Variation of local porosity results in the change of permeability. In turn, the change will affect the flow field behaviors such as the velocity and dynamic viscosity of the fluid phase. Flow field modifications, hence, control the transport of colloid, and clogging phenomena may occur around the injection point.

2.3 Flow Field

In this study, we assume that deposition of the particles in the aquifer occurs slowly and the groundwater flow is close to the steady-state in a confined aquifer, that is usually written as (Bear, 1972)

$$\nabla.(T\nabla h) = q_0 \delta(\boldsymbol{x} - \boldsymbol{x}_0) \quad , \tag{6a}$$

subjected to the following boundary conditions

$$h = h_D \qquad at \ \Gamma_D \quad , \tag{6b}$$

where T denotes the heterogeneous transmissivity (m^2/s), h is the hydraulic head (m), q_0 represents the injection source term (m^2/s) at various well positions x_0, δ is Kronecker delta.

Assuming that the aquifer has a constant thickness b (m), hence

$$T = b \, K \, , \tag{7}$$

where K (m/s) is the hydraulic conductivity, related to the intrinsic permeability k (m^2) by

$$K = k \frac{g\rho_w}{\mu} \, , \tag{8}$$

with ρ_w (kg/m^3) and μ (kg/m/s) are the density and the dynamic viscosity of fluid, respectively; g (m/s^2) is the gravity acceleration.

The intrinsic permeability is in relationship with the porosity as proposed in (Carman, 1997; Kozeny, 1927) and can be rewritten as follows

$$k = k_0 \frac{(1 - \phi_0)^2}{\phi_0^3} \frac{\phi^3}{(1 - \phi)^2} \, , \tag{9}$$

where k_0 is the initial permeability (m^2); ϕ_0 and ϕ are initial and instantaneous porosities of the medium (-). However, the Carman-Kozeny formulation is not the only one to link hydraulic conductivity to the deposition and detachment processes; other empirical equations have also been used, in which the fitting parameters are obtained using experiments (Yang, et al., 2019; Vaz, et al., 2016).

The dynamic viscosity of the fluid evolves proportionally to the colloid concentration and can be accessed by Einstein's formula (Einstein, 1906)

$$\mu = \frac{\mu_0}{(1 - \frac{M}{\rho_s c})^{2.5}} \quad , \tag{10}$$

where μ_0 is initial dynamic viscosity.

For low concentration of the dilute suspension, the first order approximation yields

$$\mu = \mu_0 \left(1 + \frac{2.5M}{\rho_s c}\right). \tag{11}$$

2.4 Coupled Inverse Problem

To monitor the evolution of the clogging effect on the transmissivity field, we implement a time-lapse inversion code, assuming that two successive transmissivity changes in time follow certain statistical characteristics expressed via a covariance function. The inverse problem is an undetermined formulation and based on minimizing the following objective function

$$L = [h^{obs} - h(s)]^T G^{-1}[h^{obs} - h(s)] + [c^{obs} - c(s)]^T W^{-1}[c^{obs} - c(s)]$$

$$+ [s^{t+\Delta t} - s^t]\Pi_{\Delta s}^{-1}[s^{t+\Delta t} - s^t] \tag{12}$$

where h^{obs} *(n×1)* is the observation hydraulic head recorded during the colloids injection, with *n* is the number of measurements; G *(n×n)* = $\sigma^2 I$, is the covariance matrix of the measurement errors, c^{obs} *(n×1)* is the measured concentration of the particles in the observed wells, W *(n×n)* = $\sigma_c^2 I$, is the covariance matrix of concentration measurement errors. s is the logarithm of the transmissivity, $s(m×1)$ = - $log_{10}(T)$ with *m* represents the number of unknown parameters, regarded as unknown field. The $s^{t+\Delta t}$ *(m×1)* and s^t *(m×1)* are parameter vectors at successive time steps. $\Pi_{\Delta s}$ *(m×m)* is the covariance matrix, derived from a geostatistical variogram that is introduced as a priori information to constraint the evolution in time of the transmissivity field; in this paper we used a Gaussian variogram :

$$\gamma(\boldsymbol{x}, t, d) = a(\boldsymbol{x}, t)\left(1 - e^{-3\frac{d^2}{r(\boldsymbol{x},t)^2}}\right), \tag{13}$$

where a(**x**,t) and r(**x**,t) are the sill and range at the position **x** and time *t*, respectively; *d* is the distance to **x**. The variation of the transmissivity neighboring the colloid injection well is the largest that

corresponds to the largest sill and it is set to a maximum value ranging from 0.1 to 0.2 in this model. The range r was chosen equal to 8m at the injected well and increase to 20m at far-away locations.

Solving the inverse problem relies on an iterative process with successive linearization of the forward problem to estimate the recent step s_{k+1}

$$s_{k+1} = s_k + \xi \Delta s \ , \tag{14}$$

where

$$\Delta s = \left[J_h^T G^{-1} J_h + \Pi_{\Delta s}^{-1}\right]^{-1} J_h^T \left(h^{obs} - h(s)\right) + \left[J_c^T W^{-1} J_c + \Pi_{\Delta s}^{-1}\right]^{-1} J_c^T \left(c^{obs} - c(s)\right), \tag{15}$$

With ξ is a scalar estimated from minimize function L by using the line search method; J_h (m×n) and J_c (m×n) are the Jacobian matrices of the hydraulic head and concentration in respect to the logarithm of transmissivity.

$$J_h = \frac{\partial h_i(s)}{\partial s_j} = \frac{h_i\left(s_k + \Delta s_j\right) - h_i(s_k)}{\Delta s_j} \ , \tag{16a}$$

$$J_c = \frac{\partial c_i(s)}{\partial s_j} = \frac{c_i\left(s_k + \Delta s_j\right) - c_i(s_k)}{\Delta s_j} \ , \tag{16b}$$

The computation of J_h and J_c adopting a finite difference technique requires to run the forward model for each perturbation Δs_j, for each iteration. Thus, the approach is very time-consuming particularly for an underdetermined inverse problem (number of unknown parameters >> number of data). To overcome this issue, we used the adjoint equations to determine the sensitivity coefficients $\partial h/\partial s$ and $\partial c/\partial s$ with the following integration (Sun & Yeh, 1990)

$$\frac{\partial h}{\partial s} = \iint_\Omega -\log 10 \left[T\nabla h\nabla \varphi_1 - KF\nabla c\nabla \varphi_2 + Kc\nabla h\nabla \varphi_2\right]d\Omega, \tag{17a}$$

$$\text{with } f = h(x)\delta(x - x_{obs})$$

$$\frac{\partial c}{\partial s} = \iint_\Omega -\log 10 \left[T\nabla h\nabla \varphi_1 - KF\nabla c\nabla \varphi_2 + Kc\nabla h\nabla \varphi_2\right]d\Omega, \tag{17b}$$

$$\text{with } f = c(x)\delta(x - x_{obs})$$

where F is a tensor with components $F_{ij} = \partial D_{ij}/\partial v_l \ \partial h/\partial x_l$ (the summation for $l = 1,2$ is implied). Other variables h, c, φ_1 and φ_2 are obtained by solving the following set of adjoint equations twice for J_h and J_c by choosing the function $f = h(x) \ \delta(x-x_{obs})$ and $f = c(x) \ \delta(x-x_{obs})$, respectively (where x_{obs} is the

location of the measurement). The adjoint problem at the steady state in a two-dimensional case is governed by (Sun & Yeh, 1990)

$$
\begin{cases}
-\nabla(T\nabla\varphi_1) - \nabla(Kc\nabla\varphi_2) + \nabla(K\boldsymbol{E}\nabla\varphi_2) & = -\dfrac{\partial f}{\partial h} \\
-\nabla(\boldsymbol{D}\nabla\varphi_2) - \boldsymbol{v}\nabla\varphi_2 - K_d\varphi_2 = -\dfrac{\partial f}{\partial c}
\end{cases}
\tag{18}
$$

with

$$
D_{ij} = \alpha_T V \delta_{ij} + (\alpha_L - \alpha_T)\frac{v_i v_j}{V} + D_m \tau \delta_{ij},
\tag{19}
$$

where α_L (m) and α_T (m) are longitudinal and transverse dispersivity, respectively; V (m/s) is the magnitude of velocity, D_m (m^2/s) is the molecular diffusion, τ is the tortuosity, and δ_{ij} is the Kronecker delta. E is a tensor with components $E_{ij} = \partial D_{il}/\partial v_j\, \partial c/\partial x_l$ (the summation for $l = 1,2$ is implied). In this study, we only focus on the determination of the transmissivity field; the transport parameters, such as dispersivities, are assumed to be known and are reported in Table 1.

The set of equations is solved using the PDE coefficient form in COMSOL and the inversion process is implemented with MATLAB. The formulation in those softwares provides a flexible solution, which could be adopted for a variety of physical problems, including the advective-diffusive equations. The model can be also coupled with a variety of boundary conditions such as Dirichlet, Neumann or mixed.

# 3   Numerical applications

In this section, we present and discuss the results of the application of the inverse protocol on theoretical cases. This discussion is built around the analysis of the algorithm's ability to retrieve the time variations of hydraulic conductivity field induced during the colloidal injections.

Before injecting the colloids in the aquifer, we should identify the initial transmissivity field of the aquifer, which is the starting point of the whole process. For this purpose, we realize a conventional sequential series of pumping tests to derive the spatial heterogeneity of this initial transmissivity field by applying a geostatistical inverse process.

Once the initial transmissivity is determined, the injections of colloids are then performed in the three wells. The evolution of the field in time and space will be estimated using directly the measurement collected during injecting the colloids in one well. We assume that the clogging will proceed slowly so that all the measurements are in a quasi-stationary state. The inverse problem will be solved first to interpret the hydraulic head data, then the hydraulic head and the concentration jointly.

3.1 Description of the case study

In this study, we used a regular array of 13 wells separated with 5m to cover a confined aquifer with heterogeneous transmissivity and porosity fields generated geostatistically with the mGstat software (Deutsch & Journel, 1997).
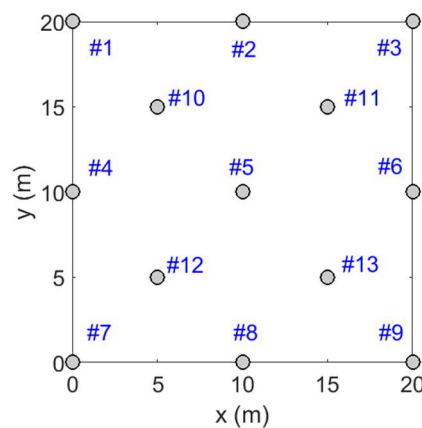
Figure 1: Arrangement of the wells, including 13 wells numbered #1-13.

The true initial fields of transmissivity and porosity used before any disturbance by the colloid injections are supposed to obey Gaussian distributions with the following characteristics $\gamma_T(r) = 1.0$ [1-exp(-r/10)] and $\gamma_\varepsilon(r) = 0.2$ [1-exp(-r/10)], respectively. The study area is bordered by the wells in a square of 20×20m discretized into 1×1m blocks (equal to 400 unknown variables) where the injections of colloids are carried out later. To limit the influence of the boundary conditions, the computed area is of 25 times larger than the study area. We consider that the effect of background gradient within the study area is negligible compared to water flow due to the injection source. The

initial transmissivity field is shown in the Figure 2 in which the transmissivity values varies between [10^{-6}, 10^{-2} m^2/s].
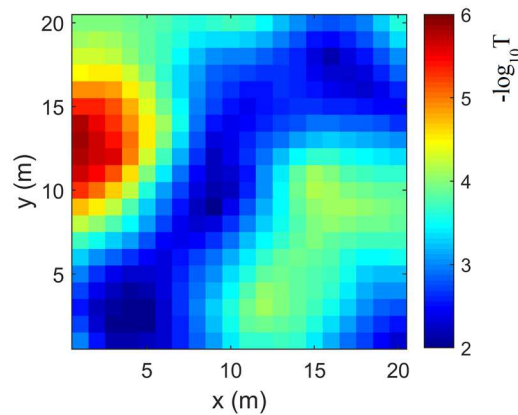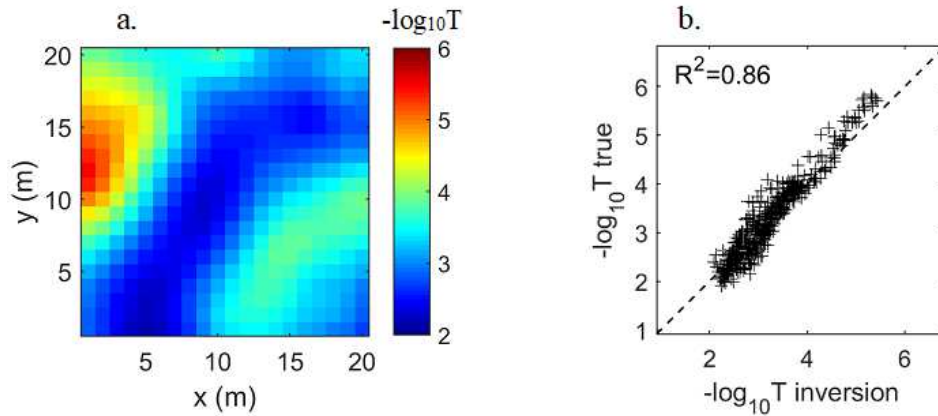

Figure 2: Initial transmissivity field in which the transmissivity varies over a range of 4 orders. Colloid injections in various wells are intended to reduce transmissivity in the conductive areas.

First, we characterize the initial transmissivity field before processing the colloid injections. A series of pumping tests with a rate of 15 m^3/day is imposed sequentially in the 13 wells, and the hydraulic head responses are numerically computed in the steady-state at various wells. Gaussian noise with $\sigma = 2\%$ of measured values is added to the data as a measurement error. The characterization of this initial field is performed by interpreting the hydraulic responses using a geostatistical inverse algorithm in which the unknown parameters of transmissivities are constrained by a geostatistical variogram. The details of this inversion solving refers to the works in (Kitanidis, 1995; Cardiff & Kitanidis, 2008). The inverse process starts from the mean of initial hydraulic transmissivity 10^{-4}m^2/s regarded as a prior information. The inversion result is shown in the Figure 3a obtained after 5 iterations and the comparison between the true and inverted fields is presented in Figure 3b.

Figure 3: Estimation of the initial transmissivity field, which represents the hydraulic features of the aquifer before the injections: a) Inverted field, b) Comparison between the true and inverted transmissivity. The inverted field reproduce the major heterogeneity of the true transmissivity field and this initial inversion will serve as the starting point in the time lapse algorithm.

The main aspect of the heterogeneity is well mapped with a certain smoothness. This estimated initial field becomes an initial input for the time-lapse inversion algorithm to image the transmissivity at the next time step that impacted by particle injections.

For this test, we use three wells to sequentially inject fine particles with low concentration. The first injection is carried out in the well #5, at the center of the medium during 60 days. In the other wells (#11 and #12), each injection lasts 40 days sequentially. This alternation of injection wells is due to a significant decrease in hydraulic conditions around the wells over time, preventing the continuation of injections. Moreover, in the remediation operations, the multiplication of pumping wells is a privileged strategy to build broader geochemical barriers for better containment of contaminated areas.

The injection process is derived from the numerical resolution of the transport and groundwater flow equations with physical properties listed in Table 1. Then, we extract the numerical measurements of the hydraulic head and colloid concentration at each well during the injection process. These data will be used in the inverse algorithm to predict the evolution of the hydraulic transmissivity.

**Table 1: Parameters used in the test of colloids injection.**

Description	Symbol	Value
Aquifer thickness	b	20m
Fluid density	ρ_w	1000 kg/m^3
Solid density	ρ_s	2600 kg/m^3
Injection flow	q_0	60 m^3/day
Injection concentration	c_0	360 mg/l
Molar mass	M	60.08 g/mol
Attachment rate	K_d	0.01 1/s
Longitudinal dispersivity	α_L	10m
Transverse dispersivity	α_T	3m
Molecular diffusion	D_m	10^{-9} m^2/s

The inverse problem deals with a parameter vector, i.e., **s**, which represents an unknown and distributed transmissivity field in space, containing hundreds of elements. The problem is undetermined, and the hydraulic data are not sufficient to arrive at a unique solution. This difficulty is generally overcome by adding in the objective function the constraints, and the prior information about the unknown parameters (Cardiff & Kitanidis, 2008) or by increasing the measurement data. In our case, we test both approaches: in the first case, we include in the objective function the time-lapse term $\mathbf{\Pi}_{\Delta s}$, to control the evolution of the transmissivity field in time and space. In the second, we combine in the inverse process the hydraulic head and concentration. The effectiveness of the additional field data is discussed later in the comparison between both results.

3.2 Time-lapse Inversion Using Only Hydraulic Head Data

To start the numerical investigation, we inject the fine particles for 60 days in the well #5 at the center of the medium. At the end of the injection process, the deposition of the fines clogs the neighborhood of the injection well leading to a reduction in hydraulic conductivity in and around the well. The resulting transmissivity at the clogging state is of around three orders of magnitude lower than the initial transmissivity (see figure 4). The hydraulic head data collected at 13 wells resulting from these hydraulic modifications are used in the time-lapse inversion algorithm to identify the zones impacted by the injection of colloids through the reconstruction of the evolution of transmissivity in time. We assume that the hydraulic measurements evolve slowly enough to be considered in a quasi-stationary state, and an error of 5% is added to the measurements to get close to real field conditions. The inversion is performed with hydraulic data sampled over two periods T = 40 days and T = 60 days. By comparison the true and estimated transmissivity fields, we can conclude that the inverse solution can reproduce the clogging phenomenon at the injected well, and that the decrease in time of transmissivity was well identified.
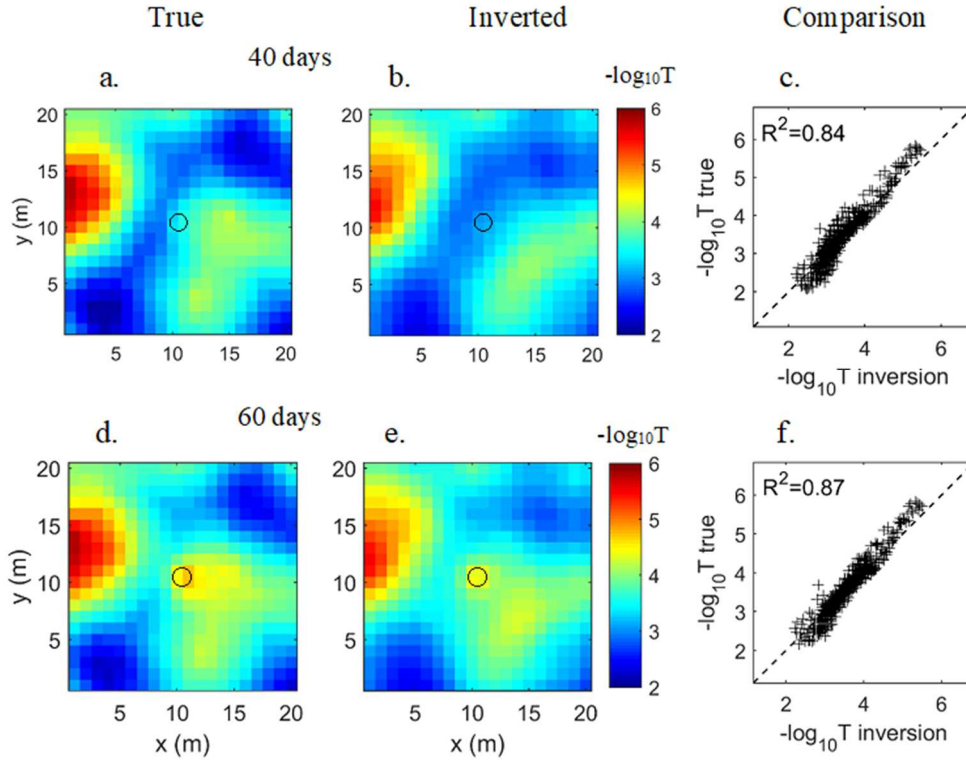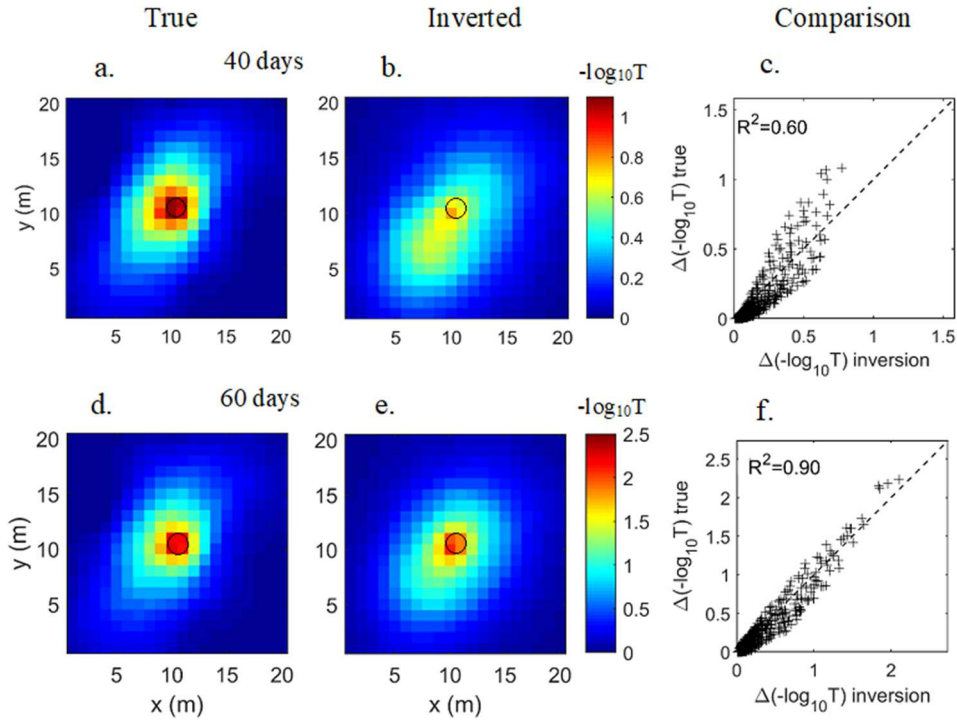
Figure 4: Injection occurs in the center of the medium (well # 5, black circle). By column, from left to right: True transmissivity field (s^t_{true}) - Inverted transmissivity filed (s^t_{inv}) - correlation between them. By row, from top to bottom: T= 40 days, T = 60 days. The inverted results highlight the main variations in hydraulic transmissivity located around the injection well.

To have a better view of the evolution of the transmissivity, we map the differences between the transmissivity field obtained at different steps of clogging and the initial field (see Eq 20). These are illustrated in Figure 5:

$$\Delta \boldsymbol{s}_{true} = \boldsymbol{s}^t_{true} - \boldsymbol{s}^{t=0}_{true} \ , \tag{20a}$$

$$\Delta \boldsymbol{s}_{inv} = \boldsymbol{s}^t_{inv} - \boldsymbol{s}^{t=0}_{inv} \ , \tag{20b}$$

with $\boldsymbol{s}^{t=0}_{true}$ and $\boldsymbol{s}^t_{true}$ are the initial true parameter and the one at time t, respectively; $\boldsymbol{s}^{t=0}_{inv}$ and $\boldsymbol{s}^t_{inv}$ are the initial inverse parameter and the one at time t, respectively.

Figure 5: Changes in the hydraulic transmissivity induced by the particle injection at the center of the medium. By column, from left to right: True field (Δs_{true}) - Inverted field (Δs_{inv}) - Comparison between them. Inverted models outline the shape of the clogging area centered on the injection well.

The representations in terms of differences provide a clearer view of the evolution of hydraulic transmissivity presented on the right side of Figure 5, on which we observe that the injections performed over 60 days permitted to reduce the transmissivity hydraulic of an order of 10^{-2} m2/s mainly around the injection wells. Inverse estimation seems to reflect this trend of evolution in the medium with variations located only around the injection well.

To highlight the advantages of the time-lapse inversion algorithm compared to the classical geostatistical algorithm without temporal variogram, we applied this latter method to inverse independently the hydraulic data collected at different periods T = 40 and 60 days by using only the spatial statistical characteristics; as prior information in objective function such as

$$L = [h^{obs} - h(\boldsymbol{s})]^T \boldsymbol{R}^{-1}[h^{obs} - h(\boldsymbol{s})] + [\boldsymbol{s} - \boldsymbol{s}_0]^T \boldsymbol{Q}^{-1}[\boldsymbol{s} - \boldsymbol{s}_0], \qquad (21)$$

370 where $\mathbf{s}_0$ denotes the mean of the unknown parameters introduced here with the covariance matrix

Q^{-1} as prior parameters (the same one used for the inversion of initial model).

Figure 6 shows the results of the geostatistical inversion scheme, which separately restructures the

transmissivity field at each time. In contrast to the time-lapse scheme, the classical algorithm failed to

map the main heterogeneities of the two fields, as shown by the true and inverse field comparison

375 curves (Figure 6). The absence of a relationship between both periods in the inverse formulation leads

to results that present no similarity between the two inverted fields, in particular in the zones not

affected by the particle injections. The temporal covariance matrix hence plays as an extra constraint

to include memory effect in the optimization process, which permits to provide realistic and

coherence changes of hydraulic properties over time. This implies an accumulation of the

380 uncertainties from the previous steps to the next estimations.
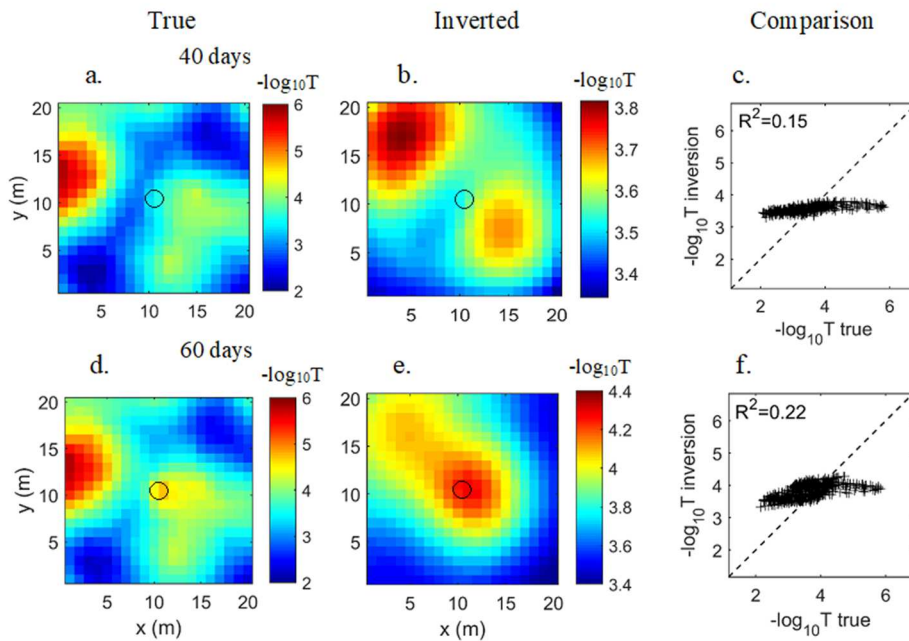
Figure 6: Geostatistical inversion of the transmissivity field using the similar hydraulic head data as Figure 4. This approach provides smooth reconstructions of hydraulic transmissivity that exhibit no similitude with the real models of transmissivity, as shown in the figure of their correlations (c and f).

In the following steps, we sequentially perform the colloid injections in the wells (#11 & #12) at the corners of the area for 40 days. These new injections significantly reduced the transmissivity values, resulting in the disappearance of the main permeable zone at the center of domain (see Figure 7, True- fields). The time-lapse inversion algorithm has also successfully delineated the main areas disturbed by the new injections (Figure 7 and 8). In these inverted fields, it can be seen that the decrease in transmissivity in the vicinity of the injected wells is visible. However, the results also show certain smoothness at the center of the injection wells. The sensitivity of the method depends on the spatial disposition of the wells, where a change of transmissivity directly induces a strong modification in the measurements compared to the areas not covered by the wells.
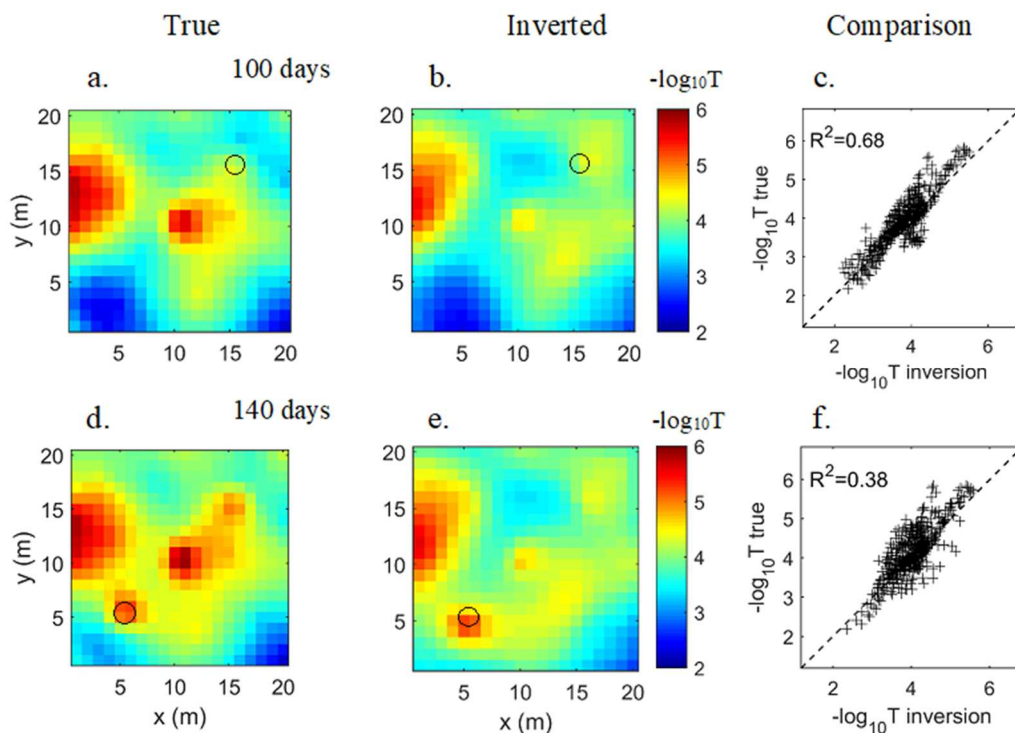
Figure 7: Transmissivity fields in logarithm (s) predicted from the hydraulic head data. Injections occur in the wells at the corners of the medium (black circle): in well #11 (subfigs a-c) and in well #12 (subfigs d-f). By column from left to right: True field (s_{true}) - Inverted field (s_{inv}) - Comparison between them. By row, from top to bottom: t = 100, 140 days. Inverted models reproduce the main aspects of the complex evolution of the transmissivity field due to colloid injections.
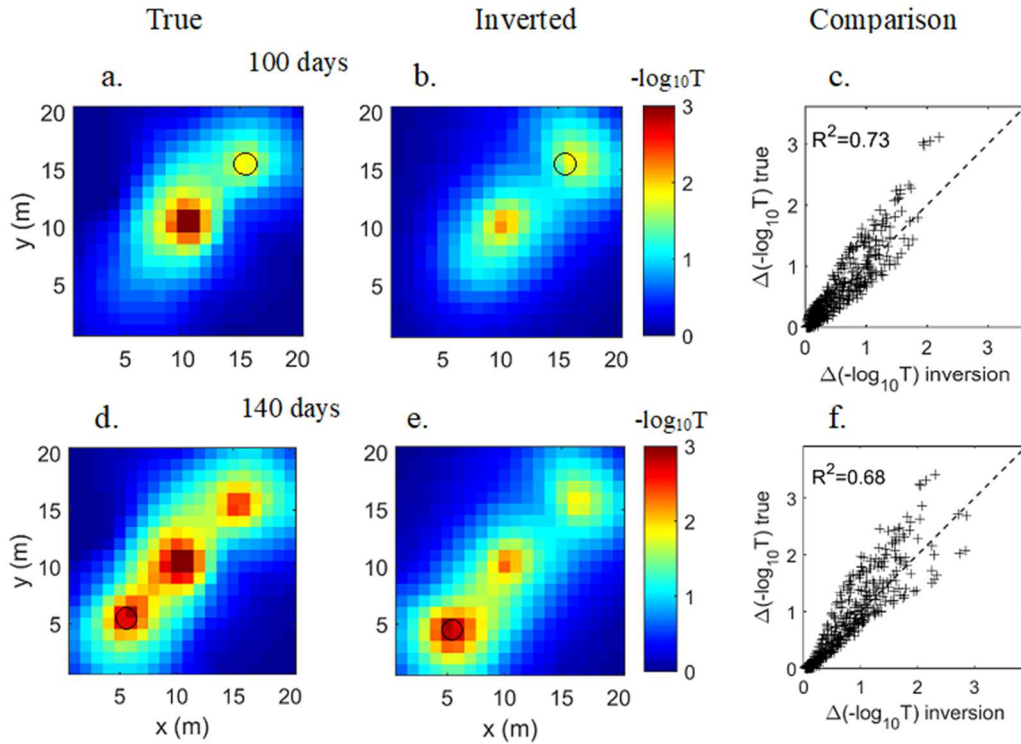
Figure 8: Changes in the hydraulic transmissivity over time. By column, from left to right: True field (*Δs*$_{true}$) - Inverted field (*Δs*$_{inv}$) - Comparison between them. By row, from top to bottom: t = 100, 140 days. The main decrease in the transmissivity field is located at the injection wells.

3.3 Time-lapse Inversion Using Both Hydraulic Head and Concentration data

In this case, the measurements of both hydraulic head and concentration in the wells are used in the inversion process. The details of the method are presented in section 2.4 with the same parametrization as that applied in the previous time-lapse inversion. The concentration data are sampled at the end of each injection when the system reaches the clogging situation, and the concentration in the injected well tends to reach a quasi-stable state. The measurement error of concentration is set at 2%.

Table 2: Correlation coefficient (R^2) between the true and inverted transmissivity fields.

| *Injection day*	*Inversion using only Hydraulic head*	*Inversion using both Hydraulic head & Concentration*

	Correlation of Transmissivity	Correlation of Difference of transmissivity	Correlation of Transmissivity	Correlation of Difference of transmissivity
60 day	0.87	0.90	0.88	0.91
100 day	0.68	0.73	0.75	0.77
140 day	0.38	0.68	0.64	0.77

We illustrate only the results of inversion at the end of each injection as shown in the Figure 9. Variations of the transmissivity field over time is detailed in the Figure 10 at 60 days, 100 days and 140 days. The comparisons between the true field and predictions, shown on the right side of Figure 10, prove some improvement of this inversion compared to the time-lapse method with only hydraulic data as shown in Figure 8, as they show less discrepancy. However, the improvement is narrow, as shown in Table 2, which is due to the fact that the concentration and hydraulic data are not independent and there is some redundancy in the information provided with the both sources of data. Hydraulic conditions play a key role in the transport of solute; consequently, it determines the distribution of the concentration field. For that reason, the importance of hydraulic data on the inverted outcomes prevails over the one of solute concentration data. The measurement of colloid concentration though enhances the precision of solutions by providing more data. The estimations over time of the joint inversion appear better in comparison to the results from the previous inversion used only hydraulic heads.
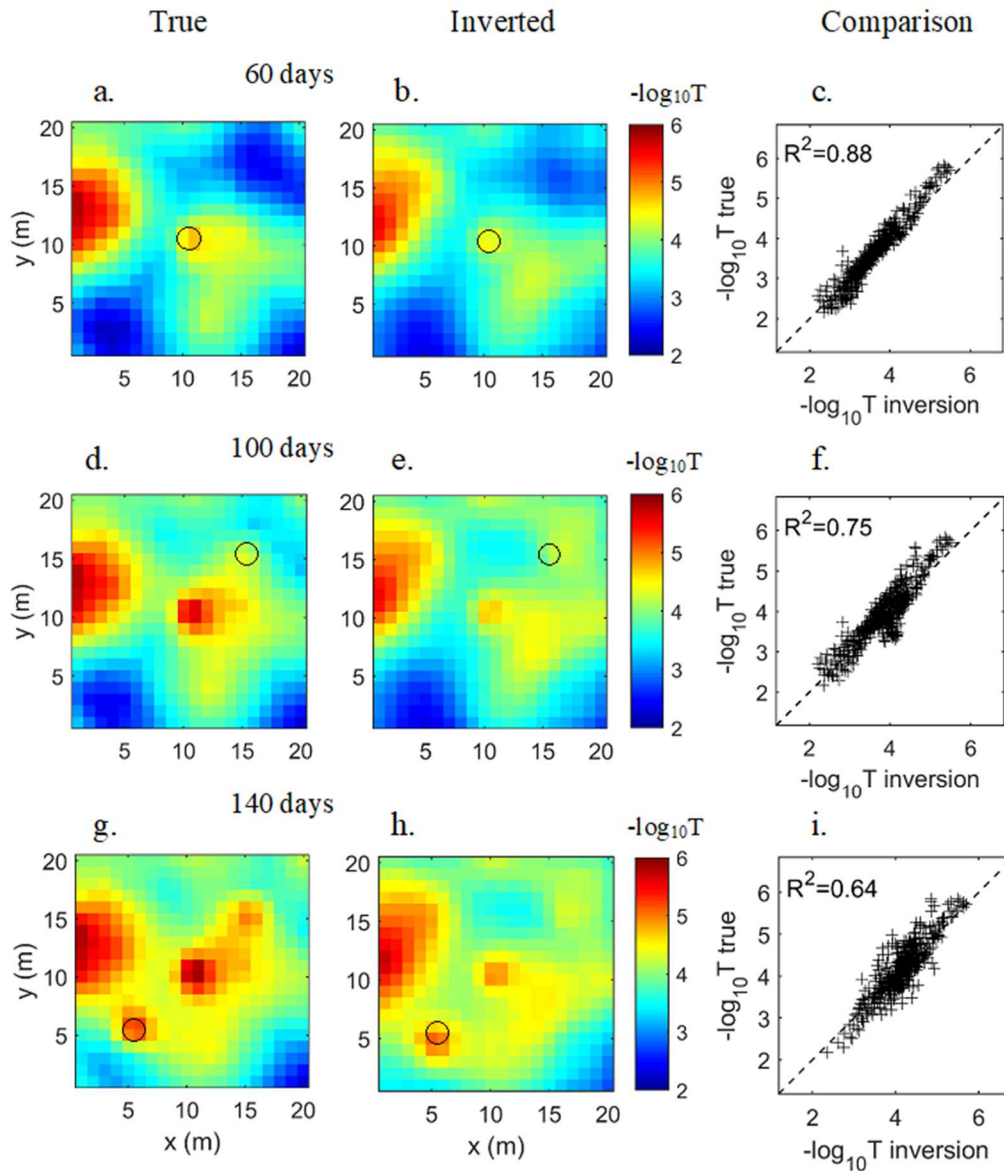
Figure 9: Transmissivity fields obtained from joint inversion of hydraulic head and concentration data. Clogging occurs in three wells (black circles): By column, from left to right: True field (s_{true}) - Inverted filed (s_{inv}) - Comparison between them. By row, from top to bottom: t = 60 days, 100 days, and 140 days. The joint inversion in time-lapse mode improves the monitoring of the evolution of hydraulic transmissivity in the medium (compared to the inversion using only the hydraulic head data).

435
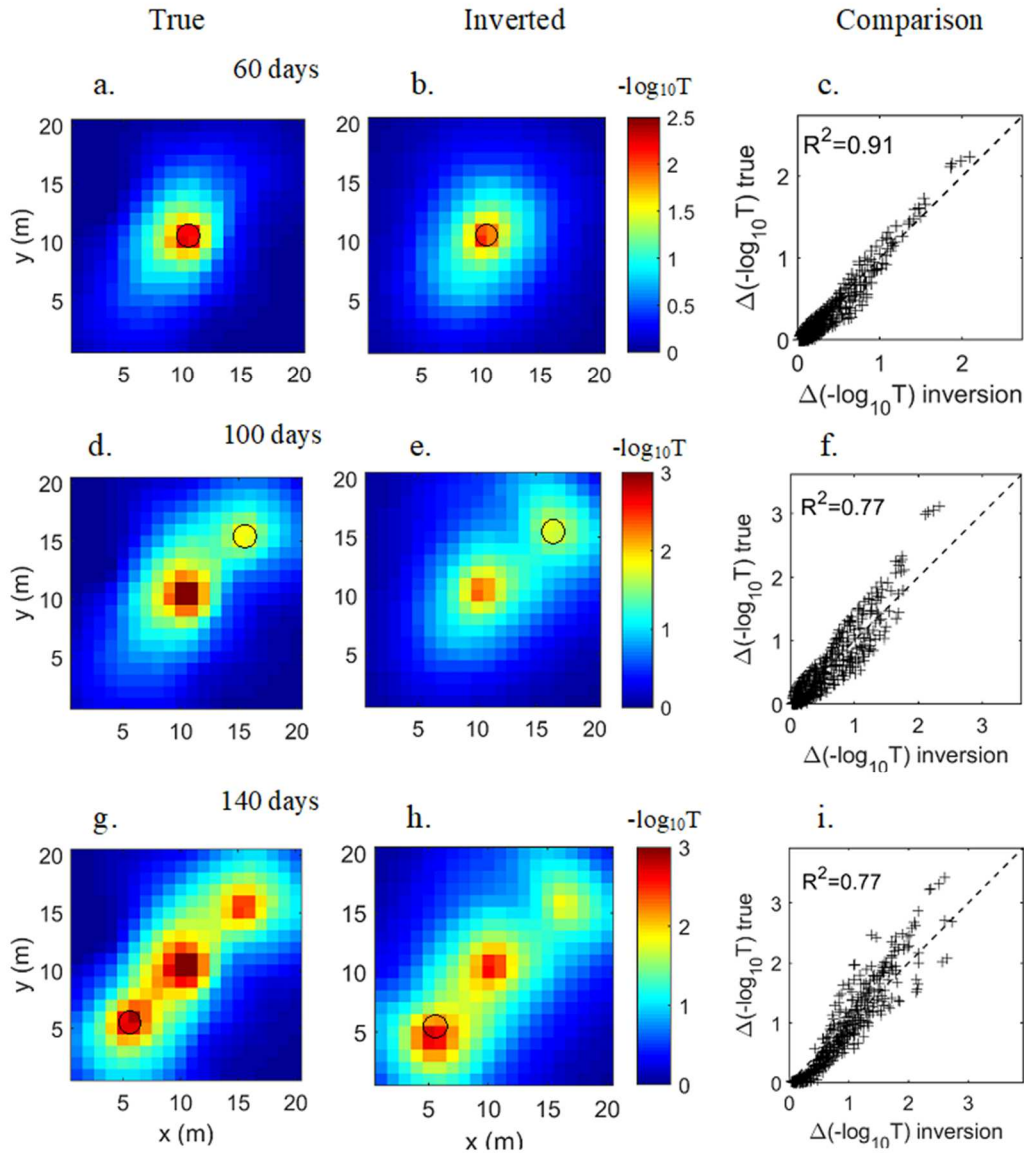
Figure 10: Comparison of true and inverted changes in hydraulic transmissivity over time shows the effectiveness of joint inversion in monitoring the effect of clogging on hydraulic conditions in the aquifer.

In addition to visual comparison, we will address a normalized misfit formula between the true field and inversion prediction for the both approaches. The misfit bases on a squared root form as following

$$\% \text{ misfit} = \sqrt{\frac{\sum \left(\frac{s_{\text{inv}} - s_{\text{true}}}{s_{\text{true}}}\right)^2}{m}} \times 100\% \tag{22}$$

where s_{inv} is the inverse parameter and s_{true} is the corresponding true parameter. The comparison between two results is presented in the Figure 11.
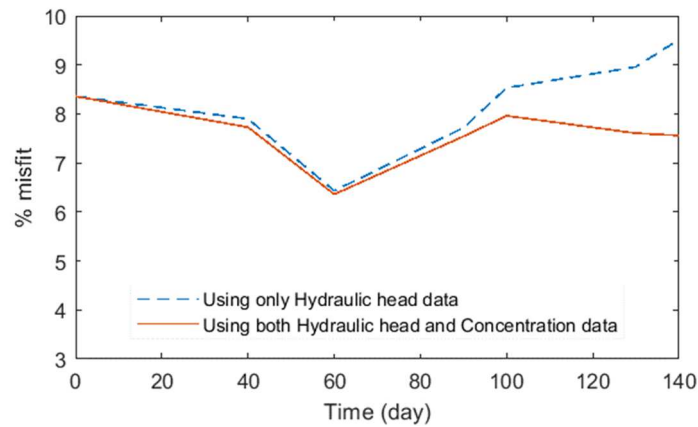
450

Figure 11: Comparison of the misfit between inverted results using only the hydraulic head data (dotted line), and coupled inversion using both the hydraulic head and concentration data (continuous line). The joint inversion model using both field measurements results in a lower misfit compared to the one using only hydraulic head data.

455   The misfit value provides a global view of the quality of the inversion process. The precision of time-lapse inversion using only hydraulic heads and coupled inversion are of the same order with the geostatistical inversion used as the starting field (at t = 0). The former inversion process uses fewer measurement data; hence, it will lose some precision and it takes a higher misfit. The accuracy of the inverse problem also depends on the number of wells used in the reconstruction and the a priori

460   constraint imposed, in our case it is the temporal covariance matrix.

4. Conclusion and Discussion

In this manuscript, we presented a new inverse approach to identify and track the changes in hydraulic transmissivity during the clogging operation from the inversion of hydraulic head and solute transport data. This hydraulic tomography algorithm is based on a time-lapse regularization, which

465   allows to control the evolution of the hydraulic transmissivity over time. This inverse problem relies on a coupled forward problem in which groundwater flow and transport equations are solved

numerically by a finite element technique to simulate the consequences of the particles injected on the modifications of the transmissivity field, and afterward on the hydraulic head data. However, for the sake of simplicity, in this article the groundwater flow equation was solved in steady state conditions.

470   The inverse problem is nonlinear and is formulated with a deterministic Quasi-Newton scheme in which the sensitivity matrices were determined from the adjoint state equations, which help to improve the efficiency of this underdetermined problem (number of data < number of unknown parameters). As many other inverse problems in geosciences, the process is still ill-posed with an insufficient number and source of data to cover faithfully the main heterogeneities of the subsurface.

475   For tackling the issue of the multiplicity of solutions, and including the memory effect in the evolution of the transmissivity field during the injections; a temporal constraint was included in the objective function. This temporal constraint was imposed to control the pattern of change of the transmissivity in time via statistical features introduced via a covariance matrix. This formulation permits to infer a current model of transmissivity from the previous one, by using it as a priori

480   information, which reduces the computation time needed to reach the convergence particularly for the deterministic algorithms and provides realistic and smooth changes of the transmissivity values. These advantages aren't offered by the traditional algorithm in which the variation of the hydraulic data at different moments are used independently to monitor the transmissivity changes. The both approaches were confronted on a hypothetical aquifer with 13 wells installed for injection of fine particles and

485   collecting hydraulic and concentration data to follow the clogging effect. The results prove that the time lapse inversions of the hydraulic data have ability to track the evolution of transmissivity in the medium which can fall to 100 order particularly around the injection wells. Therefore, this significant deterioration of hydraulic conditions around the wells reduces the effectiveness of the injection, which pushes us to use another well for the injections and the process was done on 3 wells in 140 days. The

490   multiplication of injection operations over time has utterly modified the initial transmissivity field, leading to the disappearance of the permeable zones. Most of these changes in the transmissivity field have been well identified from the inversion of the hydraulic data alone or in combination with the concentration data.

However, the joint inversion of hydraulic and concentration data has brought some improvements in the reconstruction of heterogeneities of the transmissivity field with respect to the individual inversion of hydraulic data. On the other hand, the application of the traditional geostatistical approach has not made it possible to describe the main variations of transmissivity values that occurred during injections.

We recall that the efficiency of time-lapse inversion to track the effect of clogging remains dependent as any type of inversion techniques to the number of wells used to collect data and the quality of the reconstruction of background (initial) transmissivity field.

We believe that the formulation of hydraulic tomography in time-lapse mode can be used as a powerful strategy in the field to track the hydraulic modifications induced by physical, chemical or biological clogging mechanisms. The monitoring of changes in hydraulic conditions can be performed by inverting only the water pressure, which remains a simple parameter to record when we have a series of monitoring piezometers in the field. The interpretation of these hydraulic head data can be achieved in a steady or transient state to derive both transmissivity and storativity parameters in 2D or hydraulic conductivity and specific storage in 3D, if the hydraulic data are sampled at different depths by isolating multiple discrete zones in the wells via Packer devices.

The accuracy of time-lapse hydraulic imaging is based on the quality and quantity of hydraulic data, i.e. the number of wells used in the survey, as well as the prior information added for limiting the number of solutions, and providing a realistic distribution of hydraulic properties, in our case are the spatio-temporal covariances. In the field conditions, the variogram parameters can be inferred using one of the approaches discussed in the literature, such as the exploitation of data from lithological, geological, hydrogeological and geophysical investigations conducted on the aquifer; or considering these parameters as unknowns in the inversion process (Jardani et al. 2012, Soueid Ahmed et al., 2018, Kitanidis and Vomvoris, 1983).

In this manuscript, we have proposed adding the colloid concentration data to hydraulic measurements to improve the hydraulic characterization. However, for a field application, the acquisition of concentration data is an expensive operation that demands either the deployment at

each well an optical probe, or multiplication of water sampling for laboratory analysis. Besides, the inverse formulation must take into account all parameters controlling the mechanisms of clogging, such as retention and detachment. In general, these parameters vary in space and time and depend on the hydrodynamic and chemical conditions of the medium, and their evaluations in the field is a challenge. Because if they are expressed as unknown parameters in the inversion process, the problem will become nonlinear and more complex due to their dependence on the water velocity. If they are considered as known parameters derived from laboratory experiments at the column scale, they can generate uncertainties for a field scale application. To overcome these complexities, we can opt for the dye-tracing test instead of tracking fine particles, which can provide additional information on the hydraulic characteristics of the aquifer without the need to include clogging mechanisms or even modifying the mathematical formulation of the joint inversion that remains valid for dye transfer. The dye-tracing test is a simple tool to set up in the field to track the hydrodynamic changes regardless the clogging causes (biological, chemical or mechanical). The geophysical methods including the self-potential, induced polarization and electrical resistivity tomography, which are very sensitive to the physicochemical modifications of the medium during the clogging, also represent an interesting alternative to enhance the monitoring of the change in hydraulic properties.

References

Abdel-Salam, A. & Chrysikopoulos, C. V., 1995. Modeling of colloid and colloid-facilitated contaminant transport in a two-dimensional fracture with spatially variable aperture. *Transport in Porous Media,* Volume 20, pp. 197-221.

Bear, J., 1972. *Dynamics of Fluids in Porous Media.* s.l.:American Elsevier.

Cardiff, M. & Kitanidis, P. K., 2008. Efficient solution of nonlinear, underdetermined inverse problems with a generalized PDE model. *Computers & Geosciences,* Volume 34, pp. 1480 - 1491.

Carman, P. C., 1997. Fluid flow through granular beds. *Chemical Engineering Research and Design,* Volume 75, pp. 32-48.

Cheng, T. & Saiers, J. E., 2009. Mobilization and transport of in situ colloids during drainage and imbibition of partially saturated sediments. *Water Resources Research,* Volume 45.

Civan, F., 2016. Modified Formulations of Particle Deposition and Removal Kinetics in Saturated Porous Media. *Transport in Porous Media,* Volume 111, pp. 381-410.

Civan, F. & Nguyen, V., 2005. Modeling particle migration and deposition in porous media by parallel pathways with exchange. In: *Handbook of Porous Media.* 2 ed. s.l.:CRC Press, Taylor & Francis, p. 457–484.

De Marsily, G., 1986. *Quantitative hydrogeology.* s.l.:Academic Press.

De Zwart, A. H., 2007. *Investigation of clogging processes in unconsolidated aquifers near water supply wells,* s.l.: Delft University of Technology.

Deutsch, C. V. & Journel, A. G., 1997. *GSLIB: Geostatistical Software Library and User's Guide.* 2 ed. s.l.:Oxford University Press.

Einstein, A., 1906. Eine neue Bestimmung der Moleküldimensionen. *Annalen der Physik,* Volume 324, pp. 289-306.

Flury, M. & Qiu, H., 2008. Modeling Colloid-Facilitated Contaminant Transport in the Vadose Zone. *Vadose Zone Journal,* 7(2), pp. 682 - 697.

Gruesbeck, . C. & Collins, R. E., 1982. Entrainment and Deposition of Fine Particles in Porous Media. *Society of Petroleum Engineers Journal,* Volume 22, pp. 847-856.

Hermans, T. et al., 2012. Imaging artificial salt water infiltration using electrical resistivity tomography constrained by geostatistical data. *Journal of Hydrology,* Volume 438-439, pp. 168 - 180.

IAEA, 2001. *Procedures and techniques for closure of near surface disposal facilities for radioactive waste,* Vienna, Austria: International Atomic Energy Agency.

Jardani, A., Revil, A. & Dupont, J. P., 2013. Stochastic joint inversion of hydrogeophysical data for salt tracer test monitoring and hydraulic conductivity imaging. *Advances in Water Resources,* Volume 52, pp. 62 - 77.

Jeong, H. Y., Jun, S.-C., Cheon, J.-Y. & Park, M., 2018. A review on clogging mechanisms and managements in aquifer storage and recovery (ASR) applications. *Geosciences Journal,* Volume 22, pp. 667-679.

Johnson, T. C. et al., 2010. Improved hydrogeophysical characterization and monitoring through parallel modeling and inversion of time-domain resistivity andinduced-polarization data. *GEOPHYSICS,* Volume 75, pp. 27-41.

Karaoulis , M. et al., 2011. Time-lapse three-dimensional inversion of complex conductivity data using an active time constrained (ATC) approach. *Geophysical Journal International,* Volume 187, pp. 237-251.

Kitanidis, P. K., 1995. Quasi-Linear Geostatistical Theory for Inversing. *Water Resources Research,* Volume 31, pp. 2411-2419.

Kitanidis, P. K., 1996. On the geostatistical approach to the inverse problem. *Advances in Water Resources,* Volume 19, pp. 333 - 342.

Kozeny, J., 1927. Über kapillare Leitung des Wassers im Boden. *Akad. Wiss. Wien,* Volume 136, pp. 271-306.

Legaz, A. et al., 2009. A case study of resistivity and self-potential signatures of hydrothermal instabilities, Inferno Crater Lake, Waimangu, New Zealand. *Geophysical Research Letters,* Volume 36.

Lohne, A. et al., 2010. Formation-Damage and Well-Productivity Simulation. *SPE Journal,* Volume 15, pp. 751-769.

McCarthy, J. & McKay, L., 2004. Colloid transport in the subsurface: past, present, and future challenges. *Vadose zone journal,* 3(2), pp. 326 - 337.

Mueller, N. C. et al., 2012. Application of nanoscale zero valent iron (NZVI) for groundwater remediation in Europe. *Environmental Science and Pollution Research,* Volume 19, pp. 550-558.

Persoff, P. et al., 1995. *Injectable barriers for waste isolation.* Portland, Oregon, s.n.

Peterson, N., 1994. *Design of a bottom impermeable barrier in conjunction with a contaminated site containment structure,* s.l.: University of Texas at Austin, Naval Postgraduate School.

Pronk, M., Goldscheider, N., Zopfi, J. & Zwahlen, F., 2009. Percolation and Particle Transport in the Unsaturated Zone of a Karst Aquifer. *Groundwater,* Volume 47, pp. 361-369.

Reddi, L. N., Ming, X., Hajra, M. G. & Lee, I. M., 2000. Permeability Reduction of Soil Filters due to Physical Clogging. *Journal of Geotechnical and Geoenvironmental Engineering,* Volume 126, pp. 236-246.

Ribeiro, A. F. et al., 2014. Occurrence of multi-antibiotic resistant Pseudomonas spp. in drinking water produced from karstic hydrosystems. *Science of The Total Environment,* Volume 490, pp. 370 - 378.

Saiers, J. E. & Hornberger, G. M., 1999. The influence of ionic strength on the facilitated transport of cesium by kaolinite colloids. *Water Resources Research,* 35(6), pp. 1713 - 1727.

Sen, T. K. & Khilar, K. C., 2006. Review on subsurface colloids and colloid-associated contaminant transport in saturated porous media. *Advances in Colloid and Interface Science,* 119(2-3), pp. 71 - 96.

Sharma, M. M. & Yortsos, Y. C., 1987. Fines migration in porous media. *AIChE Journal,* Volume 33, pp. 1654-1662.

Short, A. S., Lowson, T. R. & Ellis, J., 1988. 234U238U and 230Th234U activity ratios in the colloidal phases of aquifers in lateritic weathered zones. *Geochimica et Cosmochimica Acta,* 52(11), pp. 2555-2563.

Soueid, A. A., Jardani, A., Revil, A. & Dupont, J. P., 2015. HT2DINV: A 2D forward and inverse code for steady-state and transient hydraulic tomography problems. *Computers & Geosciences,* Volume 85, pp. 36-44.

Strutz, T. J., Hornbruch, G., Dahmke, A. & Köber, R., 2016. Effect of injection velocity and particle concentration on transport of nanoscale zero-valent iron and hydraulic conductivity in saturated porous media. *Journal of contaminant hydrology,* Volume 191, pp. 54-65.

Sun, N., Elimelech, M., Sun, N.-Z. & Ryan, J. N., 2001. A novel two-dimensional model for colloid transport in physically and geochemically heterogeneous porous media. *Journal of Contaminant Hydrology,* Volume 49, pp. 173 - 199.

Sun, N.-Z. & Yeh, W. W.-G., 1990. Coupled inverse problems in groundwater modeling: 1. Sensitivity analysis and parameter identification. *Water Resources Research,* Volume 26, pp. 2507-2525.

Torkzaban, S. et al., 2015. Colloid release and clogging in porous media: Effects of solution ionic strength and flow velocity. *Journal of Contaminant Hydrology,* Volume 181, pp. 161 - 171.

Vaz, A., Maffra, D., Carageorgos, T. & Bedrikovetsky, P., 2016. Characterisation of formation damage during reactive flows in porous media. *Journal of Natural Gas Science and Engineering,* Volume 34, pp. 1422 - 1433.

Wang S. & Civan F., 2005a. Model Assisted Analysis of Simultaneous Paraffin and Asphaltene Deposition in Laboratory Core Tests. *Journal of Energy Resources Technology,* Volume 127, pp. 318-322.

Wang, S. & Civan, F., 2005b. Modeling Formation Damage by Asphaltene Deposition During Primary Oil Recovery. *Journal of Energy Resources Technology,* pp. 310-317.

Yang, S. et al., 2019. Characterisation of fines migration system using laboratory pressure measurements. *Journal of Natural Gas Science and Engineering,* Volume 65, pp. 108 - 124.

Yeh, W. W.-G., 1986. Review of Parameter Identification Procedures in Groundwater Hydrology: The Inverse Problem. *Water Resources Research,* Volume 22, pp. 95-108.

Zimmerman, D. A. et al., 1998. A comparison of seven geostatistically based inverse approaches to estimate transmissivities for modeling advective transport by groundwater flow. *Water Resources Research,* Volume 34, pp. 1373-1413.